

The Shape of Poor Groups of Galaxies

M. Plionis^{1,2}, S. Basilakos², H.M. Tovmassian¹

¹ *Instituto Nacional de Astrofísica Óptica y Electrónica, AP 51 y 216, 72000, Puebla, Pue, México*

² *National Observatory of Athens, I. Metaxa & B. Pavlou, Lofos Koufou, Palaia Penteli, 15236, Athens, Greece*

27 October 2018

ABSTRACT

We estimate the distribution of intrinsic shapes of UZC-SSRS2 groups of galaxies from the distribution of their apparent shapes. We measure the projected group axial ratio using the moments of their discrete galaxy distribution. Then using the non-parametric kernel method to estimate the smooth apparent axial ratio distribution we numerically invert a set of integral equations to recover the corresponding intrinsic distribution under the assumption that groups are either oblate or prolate spheroids. We find that the prolate spheroidal model fits very well the UZC-SSRS2 group distribution with a true mean axial ratio $\langle\beta\rangle \simeq 0.3$ and $\sigma_\beta \simeq 0.15$. This shows that groups of galaxies are significantly more elongated, both on the plane of the sky and in 3 dimensions, than clusters of galaxies. The poorest groups that we consider, those with 4 members, are even more elongated than the overall population with 85% of the groups having $\beta \lesssim 0.4$.

Key words: galaxies: galaxies: groups: general

1 INTRODUCTION

In Cold Dark Matter models, structure formation evolves in a hierarchical fashion with aggregation of smaller mass units along large-scale anisotropic structures. Since virialization processes tend to sphericalize initial anisotropic distributions of matter, the shape of cosmic structures is related to their formation processes and evolutionary stage and thus it is extremely important to unambiguously determine their intrinsic shapes.

Apart from disk galaxies all cosmic structures on larger scales appear to be dominated by prolate like shapes. This has been shown to be the case for clusters of galaxies (cf. Carter & Metcalfe 1980; Plionis, Barrow & Frenk 1991; Cooray 1999; Basilakos, Plionis & Maddox 2000) as well as for superclusters which show a predominance of filamentary like shapes both observationally, theoretically and in Cosmological N-body simulations (cf. Zeldovich, Einasto & Shandarin 1982; Shandarin & Zeldovich 1983; Broadhurst et al. 1990; de Lapparent, Geller & Huchra 1991; Plionis, Jing & Valdarnini 1992; Jaaniste et al 1998; Sathyaprakash et al. 1998; Valdarnini, Ghizzardi & Bonometto 1999; Basilakos, Plionis & Rowan-Robinson 2001). In the case of Hickson or Shakhbazian compact groups it has been shown that they are even flatter than clusters and most probably prolate-like configurations with typical true axial ratios ~ 0.3 (Vardanian & Melik-Alaverdian 1978; Hickson et al. 1984; Malykh & Orlov 1986; Oleak et al. 1995).

It is obvious that the intrinsic shape of cosmic structures can be lost when projected on the plane of the sky

and therefore it is important to deal with such and other systematic effects that can hide the true shape of cosmic structures. Different studies have attempted to recover the distribution of intrinsic shapes from the corresponding apparent distribution using inversion techniques based on the assumption that their orientations are random.

The plan of the paper is the following: In Section 2 we describe the group sample that we use. We attempt to identify the extent of projection contamination and we describe the projected shape determination method. In Section 3 we invert the projected axial ratio distribution and recover the corresponding intrinsic one. The discussion and our conclusions are presented in Section 4.

2 PROJECTED POOR GROUP SHAPES

We use the recent UZC-SSRS2 group catalogue (Ramella et al 2002) which is based on the Updated Zwicky Catalogue (UZC; Falco et al. 1999) and the Southern Sky Redshift Survey (SSRS2; da Costa et al 1998), to measure the projected group shape distribution and hence attempt to estimate their intrinsic shape. The catalogue has a sky coverage of 4.69 sr, it is limited to $m_B \simeq 15.5$ and contains 1168 groups of galaxies exceeding a number density contrast threshold of $\delta\rho/\rho = 80$. The group catalogue was constructed using the well-known friends of friends algorithm with a linking parameter that scales with increasing redshift, in order to take into account the galaxy selection function.

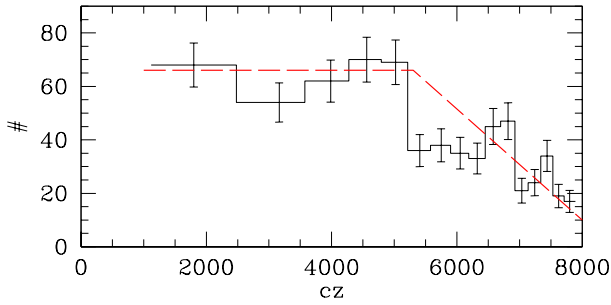


Figure 1. The group number density in equal volume shells. Note that we plot the number density only for $cz > 1800 \text{ km s}^{-1}$. At smaller distances there is a local excess in detected groups. The dashed line shows a crude fit to the data

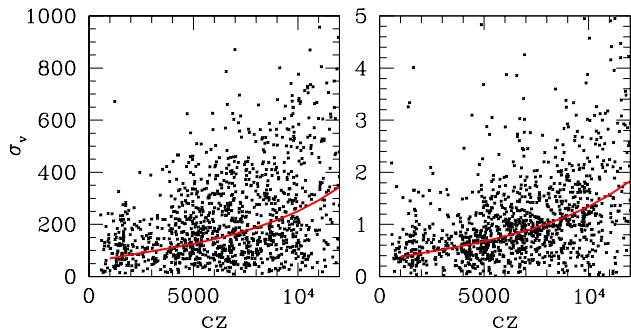


Figure 2. The dependence of the group velocity dispersion (left panel) and maximum intergalaxy separation in $h^{-1} \text{ Mpc}$ (right panel) on the group redshift. The continuous lines represent the dependence of the line-of-sight velocity (V_L ; left panel) and the projected separation (D_L ; right panel) galaxy pair linking parameters on the redshift.

In order to have a representative sample of the true underlying group population, we have chosen to study those groups the number density of which, within some limiting redshift, is relatively constant. We have derived the group number density as a function of redshift in equal volume shells (see Fig. 1) and we have found that it is roughly constant out to $cz \sim 5500 \text{ km s}^{-1}$, which we choose as our limit. Within this velocity limit we have a total of 245 groups with 4 or more members.

In Fig. 2 we present the group's velocity dispersion as well as their maximum intergalaxy separation as a function of redshift. A strong z -dependence is evident, although such dependence is rather weak within $\sim 5500 \text{ km s}^{-1}$. What is the cause of this redshift trend?

We note that in order for the Ramella et al. (2002) algorithm to identify groups having the same limiting density contrast at the different distances, it was necessary to take into account the drop with redshift of the galaxy space density which is due to the magnitude limit of the parent galaxy catalogue. The way this is accomplished is by increasing with redshift the linking parameters, used to identify the group members. The Ramella et al (2002) algorithm, like most

others, uses two linking parameters; one that links pairs of galaxies below some projected separation, i.e., $D_{12} < D_L$, and one that links galaxies with line-of-sight velocity differences below so threshold, i.e., $V_{12} (\equiv |V_1 - V_2|) < V_L$. Therefore in order to keep the limiting density enhancement of the detected groups constant it is necessary to scale the linking parameters by a distant dependent quantity that compensates, as discussed before, for the drop of the selection function of the parent galaxy population. For example, Ramella et al (2002) use the following scaling:

$$D_L = D_o R \quad \text{and} \quad V_L = V_o R,$$

where

$$R = \left(\frac{\int_{L_{min}}^{L_{max}} \Phi(L) dL}{\int_{L_{min}(r)}^{L_{max}} \Phi(L) dL} \right)^{1/3}$$

with $\Phi(L)$ the galaxy luminosity function, L_{min} the faintest luminosity at which galaxies with the limiting magnitude of the catalogue can be visible at the fiducial velocity used (1000 km/sec) and $L_{min}(r)$ the faintest luminosity at which galaxies with the limiting magnitude of the catalogue can be visible at the distance r . In Figure 2 we also plot by continuous lines the values of V_L (multiplied by a factor 1/5) and D_L (multiplied by 1.5) in the corresponding plots, which evidently follow the redshift trend observed in the data.

The apparently good correlation between the increase with redshift of the size and velocity dispersion of groups and the corresponding increase of the group linking parameters suggests that the bias is introduced by the algorithm itself, especially by the way it deals with the drop of the galaxy redshift selection function. The fact that groups of galaxies are clustered (eg. Zandivarez, Merchán & Padilla 2003 and references therein) implies that the increase with redshift of the group linking parameters may increasingly include, as part of the identified groups, galaxies belonging to neighbouring structures; a fact which will affect both the size and velocity dispersion of the resulting groups. This systematic bias could be quantified with the use of simulations but it is out of the scope of the present work.

We conclude that the probability that the groups identified constitute a homogeneous and biased free sample as well as that they constitute real dynamical entities, decreases with redshift.

2.1 Shape determination methods

We have used two methods to determine the group shapes. The first one is according to Rood (1979), by which the axial ratio, $q \equiv (b/a)$, is such that a is the angular distance between the most widely separated galaxies in the group, and b is the the sum of the angular distances b_1 and b_2 of the most distant galaxies on either side of the line a joining the most separated galaxies. The second one is the moments of inertia method (cf. Basilakos et al 2000 and references therein). In Fig. 3 we compare the results of the two methods. It is evident that they both provide equivalent axial ratios, except in a few cases where the position of the largest pair separation, used to determine a in the first method, is strongly asymmetrical with respect to the rest of the galaxies of the group (the outliers in the figure).

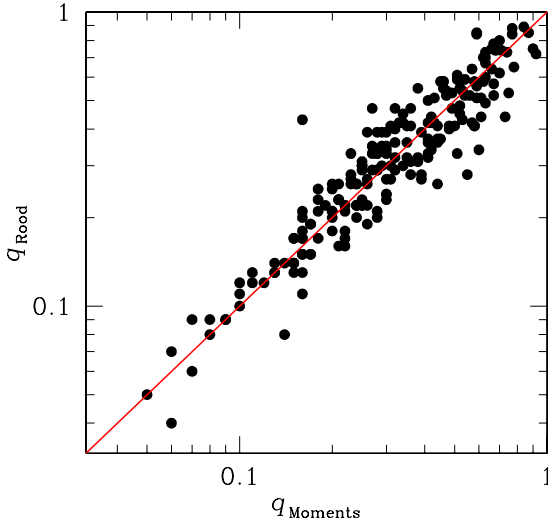


Figure 3. Comparison of the group axial ratio determined using the moments of inertia and Rood's (1979) methods.

In what follows we will use the results of the more robust moments of inertia method. Due to the slightly more complicated nature of this method, we describe it in more details below. Firstly, the galaxy equatorial positions are transformed into an equal area coordinate system, centered on the group center of mass, using: $x = (\alpha_g - \alpha_{gr}) \times \cos(\delta_{gr})$ and $y = \delta_g - \delta_{gr}$, where subscripts g and gr refer to galaxies and the groups, respectively. We then evaluate the moments:

$$\begin{aligned} I_{11} &= \sum_i w_i (r_i^2 - x_i^2) \\ I_{22} &= \sum_i w_i (r_i^2 - y_i^2) \\ I_{12} &= I_{21} = - \sum_i w_i x_i y_i \end{aligned} \quad (1)$$

with w_i the statistical weight of each point (in our case $w_i = 1$) and r_i the distance of the i^{th} galaxy from the group center of mass. Note that because the inertia tensor is symmetric we have $I_{12} = I_{21}$. Diagonalizing the inertia tensor

$$\det(I_{ij} - \lambda^2 M_2) = 0 \quad (M_2 \text{ is } 2 \times 2 \text{ unit matrix.}) \quad (2)$$

we obtain the eigenvalues λ_1, λ_2 , from which we define the principal axial ratio of the configuration under study by: $q = \lambda_2/\lambda_1 \equiv b/a$, with $\lambda_1 > \lambda_2$. The corresponding eigenvectors provide the direction of the principal axes.

2.2 Projection effects

Random projections of field galaxies could appear as groups of galaxies, which however would have no relation to dynamical entities. We have performed Monte-Carlo simulations ($N_{sim} = 10000$) and found that sets of 4 points uniformly distributed within a sphere and projected on a plane give a nearly Gaussian q -distribution with $\langle q \rangle \simeq 0.6$ and $\sigma_q \simeq 0.18$, while for sets of 10 points the corresponding values are $\langle q \rangle \simeq 0.72$ and $\sigma_q \simeq 0.13$ respectively, significantly

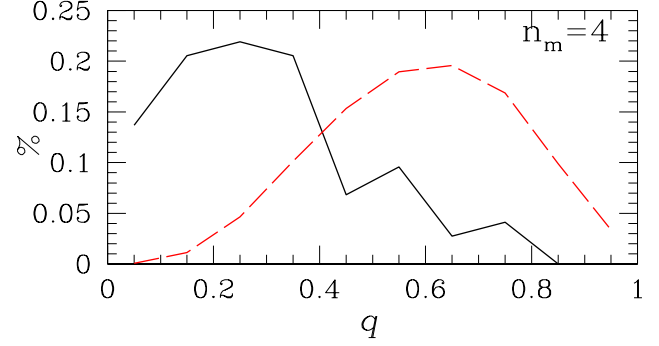


Figure 4. Comparison of the axial ratio distribution of the groups with 4 members (continuous line) with the corresponding distribution of random Monte-Carlo groups (dashed line).

larger than the observed case (see Table 1). As an example we compare in Fig. 4 the axial ratio distribution of our groups (having 4 galaxy members) with the corresponding Monte-Carlo random realizations. The difference is evident. However, this does not preclude the possibility of projection effects altering the apparent shape and the dynamical parameters of real groups.

Ramella, Pisani & Geller (1997) and Diaferio et al. (1999) based on either geometrical or N-body simulations and reproducing the group identification procedure have found that between 70% and 80% of the UZC-SSRS2 groups should be real dynamical entities, while the rest are expected to be the result of superpositions of field galaxies. Such a fraction of false groups, however, could be a serious problem for studies of the group dynamical properties, and thus should be investigated in detail.

Indeed, during our eye-balling process of verifying the group shape measurements, we encountered some cases with “strange” positional and velocity configurations, which appeared indeed to be the results of projection effects. This prompts us to check the most probable candidates of being fake groups, those with a relatively high-velocity dispersion. One such example is the group UZC269, containing four galaxies, three of which (forming a straight line) have $\langle v \rangle \simeq 4450 \text{ km s}^{-1}$ and velocity dispersion $v_\sigma \simeq 200 \text{ km s}^{-1}$, while the fourth galaxy has a velocity $4\sigma_v$ lower than $\langle v \rangle$. Another example is UZC156 with 6 members and an overall $\sigma_v = 647$. However, the total projected size of the group is $\approx 2.0 \text{ Mpc}$ while it can be separated in both velocity space and on the plane of the sky, in two triplets having $\langle v \rangle = 5200 \pm 290 \text{ km s}^{-1}$ and $\langle v \rangle = 4200 \pm 195 \text{ km s}^{-1}$. Other fake cases appeared to contain two independent groups or pairs of galaxies, with large velocity and/or spatial separations.

Of course the probability of a group being false is inversely proportional to the group galaxy membership, n_m . Random projections will affect significantly more the apparent characteristics (dynamical and morphological) of small groups rather than large ones and for this reason we have decided to exclude from our study groups with $n_m = 3$, exactly due to their *a priori* high probability of being chance projections and not real physical systems (see also Focardi & Kelm 2002).

Table 1. The median axial ratio, \bar{q} , and the median value of the maximum intergalaxy separation, \bar{a} (in h^{-1} Mpc), of the different membership UZGC groups with $cz < 5500$ km s $^{-1}$ (after exclusion of candidate false groups).

n_m	N	$\langle z \rangle$	\bar{q}	\bar{a}
4	72	0.0115	$0.27^{+0.06}_{-0.08}$	$0.54^{+0.11}_{-0.07}$
5-10	108	0.0113	$0.36^{+0.09}_{-0.08}$	$0.81^{+0.17}_{-0.15}$
all	210	0.0113	$0.36^{+0.11}_{-0.08}$	$0.77^{+0.26}_{-0.16}$

Furthermore, we have devised an objective algorithm in an attempt to single out candidate false groups having $n_m = 4$ and 5 (which are those affected the most). We will present this algorithm in an accompanying paper, which deals with the dynamics of groups (Tovmassian & Plionis 2003 *in preparation*). Here we only present the basic assumption on which the algorithm is based, which is that the probability of a group being false increases with increasing deviation of its member velocities from a Gaussian distribution having mean and variance the observed group values. We find in total 20 and 15 groups with $n_m = 4$ or 5, respectively that are probably the result of superpositions of galaxies. Note that these groups constitute a relatively small fraction ($\sim 14\%$) of the sample of 245 groups, less than the expected number of false groups, according to Ramella et al. (2002).

We have also tested our results (presented in section 3) by including these groups and found that indeed they do create problems in the inversion from the projected to the intrinsic 3D axial ratio distribution (they cause the inverted distribution for the prolate case to have unphysical negative values; see section 3).

Since the probability of a group being affected by projections is inversely proportional to n_m , we will present results also separately for groups with $n_m = 4$ and $4 \leq n_m \leq 10$.

2.3 Mean group shape parameters

The summary of the main structure parameters of the different membership samples of groups is presented in Table 1. The first and second columns give the group membership, n_m , and the number N of such groups, respectively, while the third and fourth columns show the median q and a (major axis) values, together with their 68% and 32% quantile values. It is evident that the considered UZC-SSRS2 groups are very elongated, significantly more than what expected from random projections of field galaxies, giving support to them being real dynamical entities. Furthermore, among these groups there are many so called chain-like groups, with q smaller than 0.20-0.30. The large number of chain-like groups, which also determines the relatively small median values of q , is similar to that of compact groups, the predominance of which was first mentioned by Arp (1973).

Note that the median q of all poor groups ($4 \leq n_m \leq 10$) is $0.33^{+0.09}_{-0.08}$. A certain correlation is apparent with the median b/a and a increasing with n_m . The increase of the major axis with n_m could have been due to the increase with redshift of the group linking parameter (see Ramella et al.

2002), a fact that induces the systematic increase with z of the group size (see Fig. 1). However, we have verified that the mean redshift (see Table 1) of each group subsample is constant and thus the above systematic effect is apparently not the cause of the observed increase of a with z .

The increase of the group sphericity could be explained as an indication of a higher degree of virialization, which is expected to be more rapid in systems containing more galaxies (mass). However, the increase of their major axis, if proven to be true, is somewhat more perplexing.

2.4 The projected axial ratio distribution

We now proceed in describing our approach of fitting the observed discrete distribution of axial ratios with the so-called kernel estimators. Here we review the basic steps of the Kernel method, following the notation of Ryden (1996) but for further extensive reviews see Silverman (1986), Scott (1992), Vio et al. (1994) and Tremblay & Merritt (1995).

Given the sample of axial ratios q_1, q_2, \dots, q_N for N groups, the kernel estimate of the frequency distribution is defined as:

$$\hat{f}(q) = \frac{1}{Nh} \sum_i^N K\left(\frac{q - q_i}{h}\right), \quad (3)$$

where $K(t)$ is the kernel function, defined so that

$$\int_{-\infty}^{+\infty} K(t)dt = 1, \quad (4)$$

and h is the “kernel width” which determines the balance between smoothing and noise in the estimated distribution. In general the value of h is chosen so that the expected value of the integrated mean square error between the true, $f(q)$, and estimated, $\hat{f}(q)$, distributions, $\int_{-\infty}^{+\infty} [\hat{f}_K(x) - f(x)]^2 dx$, is minimised (cf. Vio et al. 1994; Tremblay & Merritt 1995). As it has been shown in different studies the choice of a kernel function, $K(t)$, among quadratic, quartic and Gaussian forms (cf. Tremblay & Merritt 1995), provide fits that differ trivially only in their asymptotic efficiencies. We have chosen a Gaussian kernel:

$$K(t) = \frac{1}{\sqrt{2\pi}} e^{-t^2/2}. \quad (5)$$

In order to obtain physically acceptable results with $\hat{f}(q) = 0$ for $q < 0$ and $q > 1$, we apply reflective boundary conditions (cf. Silverman 1986; Ryden 1996), replacing the Gaussian kernel with:

$$K(q, q_i, h) = K\left(\frac{q - q_i}{h}\right) + K\left(\frac{q + q_i}{h}\right) + K\left(\frac{2 - q - q_i}{h}\right), \quad (6)$$

which also ensures the correct normalization, $\int_0^1 \hat{f}(q) dq = 1$.

In Figure 5 we present the projected axial ratio distributions for the different membership groups (circles), as indicated in the different panels, with their Poisson 1σ error bars, while the solid lines shows the kernel estimate \hat{f} for the appropriate width, h .

3 TRUE GROUP SHAPES

In order to find the intrinsic axial ratio distribution assuming that groups are either oblate or prolate spheroids, we

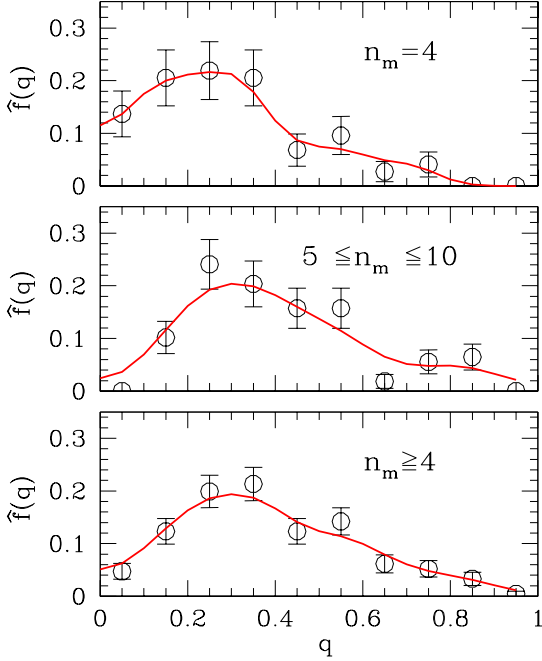


Figure 5. The apparent axial ratio distributions for different group membership. The solid line is the smooth fit from the non-parametric kernel estimator.

use an inversion method, described below. Although there is no physical justification for the restriction to oblate or prolate spheroids, it greatly simplifies the inversion problem. Furthermore, if groups are a mixture of the two spheroidal populations or they have triaxial configurations then there is no unique inversion (Plionis, Barrow & Frenk 1991).

The relation between the apparent and intrinsic axial ratios, is described by a set of integral equations first investigated by Hubble (1926). These are based on the assumptions that the orientations are random with respect to the line of sight, and that the intrinsic shapes can be approximated by either oblate or prolate spheroids. Writing the intrinsic axial ratios as β and the estimated distribution function as $\hat{N}_o(\beta)$ for oblate spheroids, and $\hat{N}_p(\beta)$ for prolate spheroids then the corresponding distribution of apparent axial ratios is given for the oblate case by:

$$\hat{f}(q) = q \int_0^q \frac{\hat{N}_o(\beta) d\beta}{(1-q^2)^{1/2}(q^2-\beta^2)^{1/2}} \quad (7)$$

and for the prolate case by:

$$\hat{f}(q) = \frac{1}{q^2} \int_0^q \frac{\beta^2 \hat{N}_p(\beta) d\beta}{(1-q^2)^{1/2}(q^2-\beta^2)^{1/2}} \quad (8)$$

Inverting equations (eq.7) and (eq.8) gives us the distribution of real axial ratios as a function of the measured distribution:

$$\hat{N}_o(\beta) = \frac{2\beta(1-\beta^2)^{1/2}}{\pi} \int_0^\beta \frac{d}{dq} \left(\frac{\hat{f}}{q} \right) \frac{dq}{(\beta^2 - q^2)^{1/2}} \quad (9)$$

and

$$\hat{N}_p(\beta) = \frac{2(1-\beta^2)^{1/2}}{\pi\beta} \int_0^\beta \frac{d}{dq} (q^2 \hat{f}) \frac{dq}{(\beta^2 - q^2)^{1/2}} \quad (10)$$

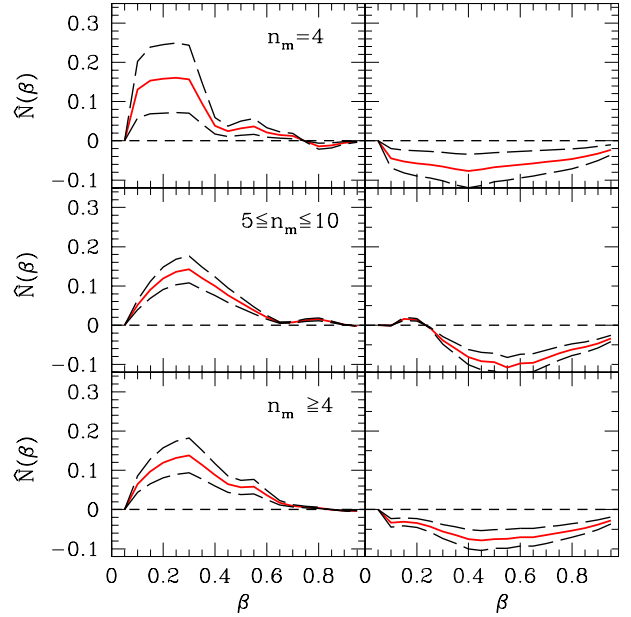


Figure 6. The distribution of the intrinsic poor group axial ratios (continuous line) and its 1σ range (broken lines) assuming that they are either prolate (left panel) or oblate (right panel) spheroids.

with $\hat{f}(0) = 0$. In order for $\hat{N}_p(\beta)$ and $\hat{N}_o(\beta)$ to be physically meaningful they should be positive for all β 's. Following Ryden (1996), we numerically integrate eq.(9) and eq.(10) allowing $\hat{N}_p(\beta)$ and $\hat{N}_o(\beta)$ to take any value. If the inverted distribution of axial ratios has significantly negative values, a fact which is unphysical, then this can be viewed as a strong indication that the particular spheroidal model is unacceptable.

In Figure 6 we present the intrinsic group axial ratio distributions. The oblate model (right panel) is completely unacceptable since it produces only negative values of the inverted intrinsic axial ratio distribution. The UZC-SSRS2 groups shape is represented well only by that of prolate spheroids which is in agreement with previous studies of albeit smaller group samples (cf. Oleak et al 1995). It is very interesting the fact that there are almost no groups with true axial ratio, $\beta \gtrsim 0.6$, i.e., there are no roundish groups while most of them are extremely elongated. The most elongated groups are the poorer ones (those with $n_m = 4$) with 85% having $\beta \lesssim 0.4$. We can crudely approximate the intrinsic prolate axial ratio distribution of all the UZC-SSRS2 groups of our sample (lower left panel of Fig. 6) by a Gaussian having $\langle \beta \rangle = 0.29$ and $\sigma = 0.16$ (see Fig. 7).

How do our group shape results compare with those of clusters of galaxies? In Figure 8 we present the distribution of intrinsic axial ratio, for the prolate case (which also is the best model for clusters; see Plionis et al 1991, Basilakos et al 2000), for both the UZC-SSRS2 groups and the APM clusters that appear to have no substructure (which means that they are probably in virial equilibrium; see Basilakos et al 2000). It is evident that groups are significantly more elongated than clusters and although there are quite a few spherical clusters, this is not the case for groups. This probably

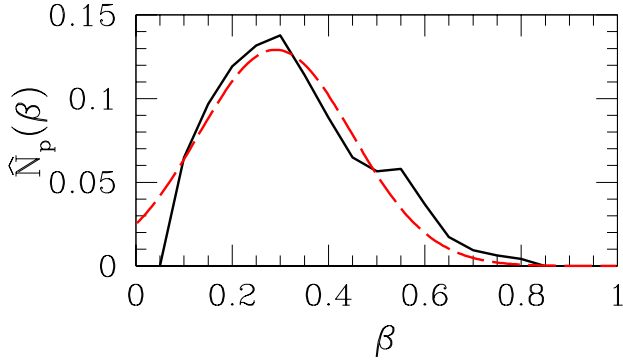


Figure 7. The intrinsic axial ratio distribution (for the prolate case) of all the UZC-SSRS2 groups of the sample analysed (continuous line) and the best Gaussian fit (broken line).

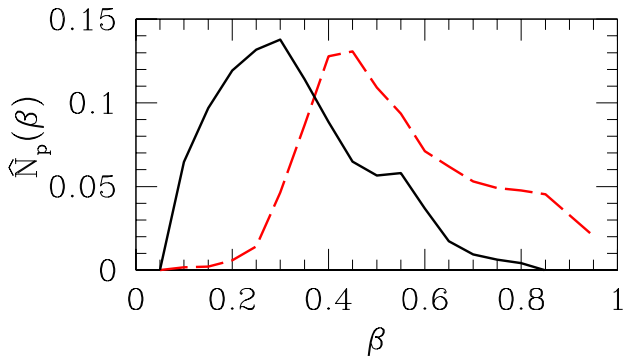


Figure 8. Comparison of the UZC-SSRS2 group (continuous line) and the APM cluster (broken line; from Basilakos et al 2000) intrinsic axial ratio distributions. Note that these distributions are based on 212 and 405 objects respectively.

implies that the cluster distribution is in a more advanced dynamical state, with violent relaxation having sphericalized the initial flattened distribution of galaxy members.

4 DISCUSSION & CONCLUSIONS

We have measured the projected axial ratio of all UZC-SSRS2 Groups of Galaxies within a volume-limited region ($cz \leq 5500$ km/sec) using the moments of the discrete galaxy distribution.

Using the nonparametric kernel procedure we obtain a smooth estimate of the apparent UZC-SSRS2 group axial-ratio distribution. The projected axial ratio distribution of the whole group sample peaks at $q \simeq 0.33$ with an extended tail towards apparently spherical groups. Assuming that the UZC-SSRS2 groups constitute a homogeneous population of either oblate or prolate spheroids, we numerically invert the apparent axial ratio distribution to obtain the corresponding intrinsic one. The only acceptable model is provided by that of prolate spheroids having an intrinsic distribution with $\langle \beta \rangle \simeq 0.29$ and $\sigma_\beta = 0.16$ (if modeled by a Gaussian). This results are in very good agreement with the analysis of 95 Shakhbazian compact groups (Oleak et al 1995) and shows

that generically poor groups of galaxies, compact or not, are extremely elongated prolate systems, much more than clusters or even elliptical galaxies.

This result supports the view by which groups form by accretion of galaxies along larger structures, like filaments, in which they could be embedded (cf. West 1994). Such an accretion process would happen preferentially along the group major axis, which should then be typically aligned with other nearby structures (groups or clusters). Such an effect is well documented for clusters (cf. Bingelli 1982; Plionis 1994, Plionis & Basilakos 2002 and references therein), but it has still to be determined for groups of galaxies.

Finally, we would like to comment on the orientation effects that the extremely elongated and intrinsically prolate nature of groups would create. When elongated groups are orientated roughly along the line of sight they will appear roughly spherical therefore having a higher velocity dispersion and smaller sizes while elongated groups seen roughly orthogonal to the line of sight will appear to have smaller velocity dispersions. This would affect relations like that between the group's X-ray luminosity - velocity dispersion and thus if not taken into account, erroneous conclusions could be reached regarding their dynamical state (see Tovmassian, Yam & Tiersch 2002; Plionis & Tovmassian 2004).

ACKNOWLEDGEMENTS

MP acknowledges funding by the Mexican Government grant No. CONACyT-2002-C01-39679. SB acknowledges the hospitality of INAOE where this work was completed.

REFERENCES

- Arp, H. 1973, *ApJ*, 185, 797
 Basilakos, S., Plionis, M., Maddox, S.J., 2000, *MNRAS*, 316, 779
 Basilakos, S., Plionis, M., Rowan-Robinson, M., 2001, *MNRAS*, 323, 47
 Bingelli B., 1982, *AA*, 250, 432
 Broadhurst, T. J., Ellis, R. S., Koo, D. C., Szalay, A. S., 1990, *Nature*, 343, 726
 Carter, D. & Metcalfe, N., 1980, *MNRAS*, 191, 325
 Cooray, R.A., 2000, *MNRAS*, 313, 783
 da Costa, L.N., et al., 1998, *AJ*, 116, 1
 de Lapparent, V., Geller, M. J., Huchra, J. P., 1991, *ApJ*, 369, 273
 Diaferio, A., Kauffmann, G., Colberg, J.M. & White, S.D.M., 1999, *MNRAS*, 307, 537
 Falco, E.E., et al., 1999, *PASP*, 111, 438
 Focardi, P. & Kelm, B., 2002, *A&A*, 391, 35
 Hickson P., Ninkov Z., Huchra P., Mamon G. A. 1984, in *Clusters and Groups of Galaxies*, Mardirossian F., Guiricin G., Mezzetti M. (eds.), 367
 Jaaniste, J., Tago, E., Einsato, M., Einsato, J., Andernach, H., Mueller, V., 1998, *A&A*, 336, 35
 Malykh, S. A., Orlov, V. V. 1986, *Astrofizika* 24, 445
 Oleak H., Stoll D., Tiersch H., MacGillivray H. T. 1995, *AJ*, 109, 1485
 Plionis M., Barrow J.D., Frenk, C.S., 1991, *MNRAS*, 249, 662
 Plionis M., Valdarnini, R., Jing, Y.P. 1992, *ApJ*, 398, 12
 Plionis, M., 1994, *ApJS*, 95, 401
 Plionis, M. & Basilakos, S., 2002, *MNRAS*, 329, L47
 Plionis, M. & Tovmassian, H.M., 2004, *A&A*, 416, 441
 Ramella, M., Pisani, A. & Geller, M. J., 1997, *AJ*, 113, 483

- Ramella, M., Geller, M. J., Pisani, A., & da Costa, L. N. 2002, AJ, 2976, 123
- Rood H. J. 1979, ApJ 233, 21
- Ryden S.B., 1996, ApJ, 461, 146
- Sathyaprakash, B. S., Sahni, V., Shandarin, S.; Fisher, K.B., 1998, ApJ, 507, L109
- Scott, D. W., 1992, *Multivariate Density Estimation for Statistics and Data Analysis* (New York: Chapman & Hall)
- Shandarin, S. & Zeldovich, Ya. B., 1983, *Comments in Astrophysics*, 10, 33
- Silverman, B. W., 1986, *Density Estimation for Statistics and Data Analysis* (New York: Chapman & Hall)
- Tovmassian, H.M., Yam, O., & Tiersch, H., 2002, ApJ, 567, L33
- Tremblay, B., & Merrit, D., 1995, AJ, 110, 1039
- Valdarnini, R., Ghizzardi, S., Bonometto, S., 1999, NewA, 4, 71
- Vardanian, R. A., & Melik-Alaverdian, Yu. K. 1978, *Astrofizika*, 14, 195
- Vio, R., Fasano, G., Lazzarin, M., Lessi, O., 1994, AA, 289, 640
- West, M. J., 1994, MNRAS, 268, 79
- Zandivarez, A., Merchn, M.E., Padilla, N.D., 2003, MNRAS, 344, 247
- Zeldovich, Ya. B., Einasto, J., Shandarin, S., 1982, *Nature*, 300, 407